

Ion Fractions and the Weak Wind Problem

Matthew Austin and Raman Prinja

Department of Physics and Astronomy, University College London,
Gower Street, London, WC1E 6BT, United Kingdom

Abstract: Some late-type O stars are observed to display anomalously weak winds. This issue and the uncertainty about the nature of wind clumping are challenges to line-driven wind theory and need resolving in order to fully understand hot stars. We describe the results from the computation of ion fractions for the various elements in O star winds using the non-LTE code CMFGEN, including parameterisations of microclumping and X-rays. Ion fractions can also be derived from fits to UV wind lines if a mass-loss rate is assumed. We discuss a project to fit unsaturated C IV lines in late O dwarfs, and show that the weak wind scenario could still be a major issue, with some values of $\dot{M}\langle q_{CIV} \rangle$ indicated to be more than an order of magnitude lower than theoretical predictions of mass-loss, and measurements from radio and optical diagnostics.

1 Introduction

There are several spectroscopic diagnostics available for measuring the mass-loss rate of O stars. Each of these has certain advantages and drawbacks, and often requires ill-determined information or parameter knowledge. In the ultraviolet, wind profiles can be matched using the SEI (Sobolev with Exact Integration) method of Lamers, Cerruti-Sola & Perinotto (1987) to yield the product of the mass-loss rate and the ion fraction of the element. The mass-loss results are therefore very dependent upon the wind ionization balance. We compiled a grid of O star models using the spherical non-LTE model atmosphere code CMFGEN (Hillier & Miller 1998), producing a variety of model types from O3 to O9.5, with different wind-clumping scenarios and with or without X-rays. These models have a large number of applications, but here we focus on the run of ion fraction with effective stellar temperature, which was derived for each clumping and X-ray scenario, to assess the possible effects of these two phenomena on the ionization balance in O star winds.

2 Model Ion Fractions

For each spectral type a set of mean ion fractions was calculated for each element, normalised to the range $0.2-0.9v_\infty$. This was done in order to ensure a direct comparison to empirical fits described in the section below, in which the very lowest and highest velocity positions are excluded so as to avoid any variable phenomena such as DACs.

Figure 1 shows the results for C³⁺ and C⁴⁺ for dwarfs, which are predicted to account for most of the total carbon population. N, O, Si, P and S were also processed but for brevity are not shown here;

they will be published separately. We focus discussion on carbon, which is pertinent to the project described in the next section. The clumping scenario is either unclumped (smooth wind, volume filling factor 1.0) or moderately clumped (with a volume filling factor of 0.1). The models with X-rays have an X-ray luminosity consistent with the relation $\log L_x/L_{bol} \sim -7$ from e.g. Nazé 2009. When changing to a clumped wind in the absence of X-rays, the higher ionization stage reduces in population at higher temperatures as recombination from higher local density forces the balance in favour of the lower stage. In general this balance appears more fragile when X-rays are implemented and the effect is greater. Bringing X-rays into the unclumped scenario shifts the balance strongly in favour of the upper stage but with a non-negligible portion still in the lower. The supposedly most detailed description of the wind (i.e. with both clumping and X-rays) yields a somewhat uncertain picture, in which it is unclear for much of the O star range whether either ion becomes dominant. A stark difference in the X-ray models is brought about by introducing moderate clumping. Whilst in the unclumped wind, the X-rays cause C^{4+} to be dominant for the whole O star range, the clumping then changes the ionization balance much more than in the non-X-ray models. In order to distinguish the most likely scenario, the profiles in the corresponding model spectra were examined and compared to observations (*IUE*, *Copernicus*, *FUSE*). For later type objects we find that it is crucial to include a treatment of X-rays to get realistic N V and O VI lines. The model profiles also seem to suggest a very low level of clumping to be most likely, implying that the bottom-left panel in Fig. 1 is that which should be used.

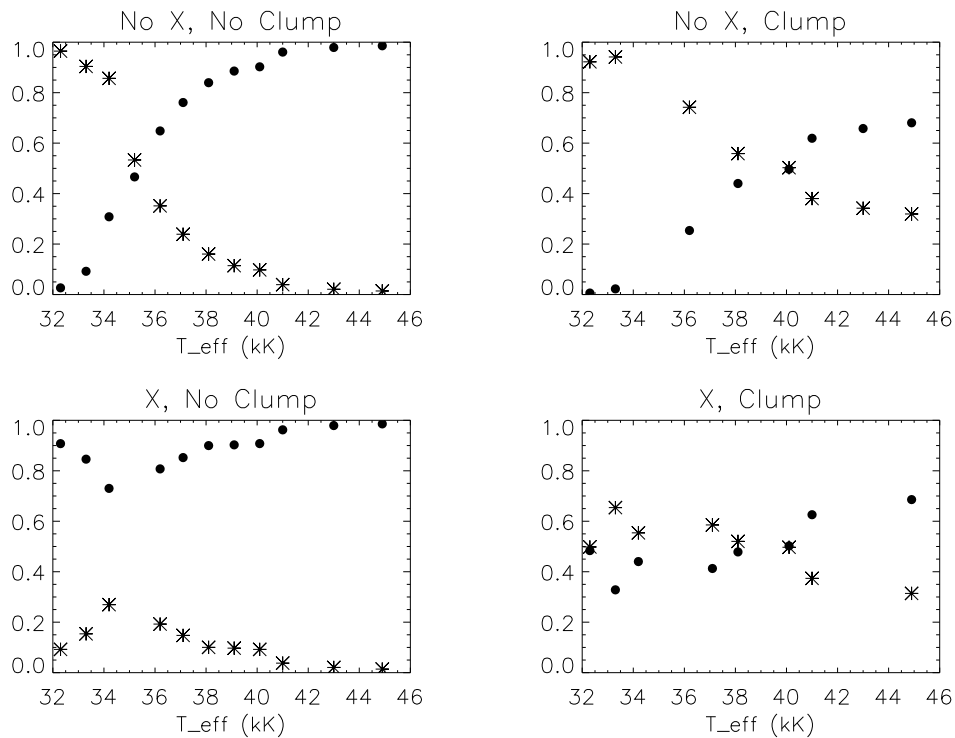


Figure 1: Ion fractions of carbon for different clumping and X-ray scenarios. Dots = C^{4+} , stars = C^{3+} .

3 Mass-loss determination

For later type dwarfs (O6-O9.5) the fraction of C^{3+} is predicted to be either ~ 0.1 or ~ 0.5 , depending on which clumping scenario is preferred. However, if canonical mass-loss rates are assumed, the ion

fractions derived from empirical modelling are rather different. C IV profiles in a sample of 30 O dwarfs were fitted using the SEI method in order to determine their $\dot{M}\langle q_{C^{3+}}\rangle$. Fig. 2 displays an example fit; that of HD41161. For all objects under investigation the quantity $\dot{M}\langle q_{C^{3+}}\rangle$ is shown in Table 1, and was generally found to be between 2 and 3 orders of magnitude lower than the theoretical predictions of \dot{M} of Vink, de Koter & Lamers (2000), which themselves are approximately in line with measures from other diagnostics (H α , radio). Even employing the X-ray and unclumped scenario, this is too large a gap once the ion fraction is taken into account. To make up for the disparity between observation and theory, $\langle q_{C^{3+}}\rangle$ would need to be in the range 0.01-0.001, and this is clearly not the case in the CMFGEN models, which show an ion fraction for C³⁺ of 0.1 or more for later type O dwarfs. The remaining discordance could be partly to do with the lack of a treatment for optically thick clumping in the SEI method. This effect has the potential to change how we interpret UV line profiles, as optically thick clumps covering the disk will change the formation of profiles (e.g. Oskinova, Hamann & Feldmeier 2007 and Sundqvist, Puls & Feldmeier 2010), however it would take a highly porous wind to bring UV-derived mass-loss rates in line with theoretical values, if only a spatial porosity is considered. Optically thick clumps as considered by Sundqvist et al. (2010) have been shown to reduce profile sizes using only moderate clumping factors, and so this may be the most likely effect to reconcile the apparent discordance. In addition, H α becomes insensitive to the mass-loss rate at later O types, and so may skew comparisons to other diagnostics. We believe there still exists a discordance between mass-loss measures, and that new diagnostics, a proper multi-wavelength approach, and a thorough treatment of optically thick clumping are required for O dwarfs.

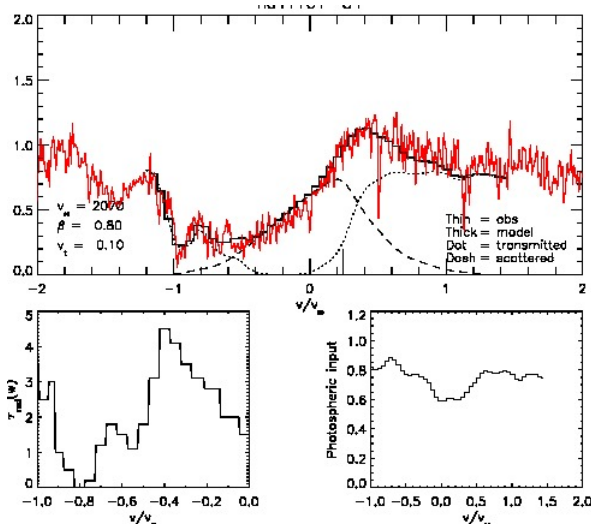


Figure 2: Fit to C IV in HD 41161. Bottom left shows the input radial optical depth; bottom right shows the photospheric contribution from TLUSTY (Hubeny & Lanz, 2003).

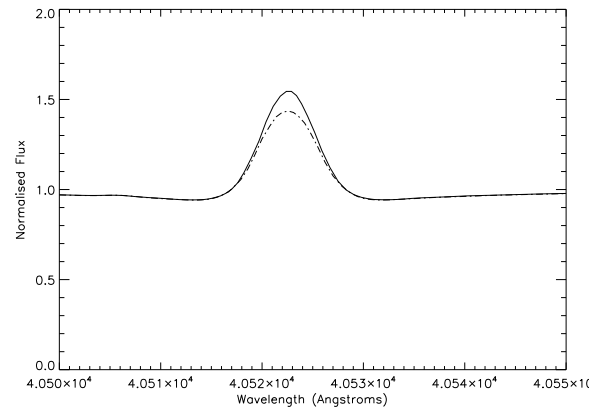


Figure 3: The region around Br α in two CMFGEN models from the grid, nominally of spectral type O9 V. Dotted: $\dot{M} = 1 \times 10^{-9}$; solid: $\dot{M} = 2 \times 10^{-9}$

To provide another diagnostic of mass-loss in weak-winded objects, we are currently gathering spectra of Br α in several Galactic O stars from the C IV investigation, using ESO-VLT/CRIRES. This line is proposed to be an excellent measure of mass-loss in weak-winded stars (Puls, Vink & Najarro 2008) and is far more sensitive in models (Fig. 3) for O dwarfs than its Balmer series counterpart. We plan to determine the Br α mass-loss rate using model atmospheres and compare it directly to the information we already have from C IV and other diagnostics, where possible.

Table 1: The product of C^{3+} fraction and mass-loss rate for the sample of O dwarfs, along with the implied ion fraction based on theoretical mass-loss rates. Effective temperatures are of equivalent CMFGEN models for the given spectral type.

HD/CPD	T_{eff} (kK)	$\log(\dot{M}\langle q_i \rangle)$	$\log \dot{M}$ (Vink)	Implied $q_i \times 10^{-3}$
5005	38.1	-9.25	-6.47	1.7
12993	38.1	-9.14	-6.36	1.7
17505	38.1	-8.86	-6.30	2.8
42088	38.1	-9.26	-6.33	1.2
54662	38.1	-9.21	-6.30	1.2
93146	38.1	-9.14	-6.42	1.9
93161B	38.1	-9.04	-6.30	1.8
101436	38.1	-9.00	-6.43	2.7
165052	38.1	-9.50	-6.30	0.6
206267	38.1	-8.99	-6.30	2.0
-59 2603	37.1	-9.96	-6.43	3.0
35619	37.1	-9.57	-6.46	0.8
36879	37.1	-9.39	-6.54	1.4
44811	37.1	-9.85	-6.43	0.4
46485	37.1	-9.17	-6.43	1.8
47839	37.1	-9.21	-6.55	2.2
48099	37.1	-9.06	-6.43	2.3
91824	37.1	-9.36	-6.43	1.2
152623	37.1	-9.07	-7.13	11.5
159176	37.1	-9.01	-6.62	4.1
41997	36.2	-9.07	-6.82	5.6
53975	36.2	-9.87	-6.50	4.3
152590	36.2	-9.63	-6.63	1.0
155806	36.2	-9.27	-6.80	3.4
14633	35.2	-10.22	-7.02	0.6
41161	35.2	-9.45	-6.62	1.5
46056	35.2	-9.98	-6.68	0.5
46966	35.2	-9.40	-6.94	3.5
48279	35.2	-8.20	-6.62	26.3
60848	35.2	-9.60	-7.02	2.6
93222	35.2	-8.99	-6.62	4.3
100213	35.2	-9.73	-6.62	0.8
101413	35.2	-9.50	-6.62	1.3
46149	34.2	-10.31	-6.86	0.4
73882	34.2	-9.34	-7.36	10.5
216532	34.2	-10.00	-6.86	0.7
75759	33.3	-10.14	-6.88	0.5
193322	33.3	-9.88	-6.88	1.0
209481	33.3	-9.78	-6.88	0.8
214680	33.3	-10.37	-6.88	0.3
34078	32.3	-10.51	-6.69	0.2
38666	32.3	-10.36	-7.05	0.5
93027	32.3	-10.24	-7.09	0.7
149757	32.3	-9.91	-6.88	0.9

Acknowledgements

MA acknowledges the use of the UCL Legion cluster for computation of models for this work, and help from John Hillier and Adam Burnley for consultation on using the code.

References

- Hillier, D. J. & Miller, D. L., 1998 ApJ, 496, 407
Hubeny, I. & Lanz, T., 2003 ASPC, 288, 51
Lamers, H. J. G. L. M., Cerruti-Sola, M., Perinotto, M., 1987 ApJ, 314, 726
Nazé, Y., 2009 A&A, 506, 1055
Oskinova, L. M., Hamann, W.-R., Feldmeier, A., 2007 A&A, 476, 1331
Puls, J., Vink, J. S., Najarro, F., 2008 A&ARv, 16, 209
Sundqvist, J. O., Puls, J., Feldmeier, A., 2010 A&A, 510, 11
Vink, J. S., de Koter, A., Lamers, H. J. G. L. M., 2000 A&A, 362, 295